galaxies

Article

A Close Binary Supermassive Black Hole Model for the Galaxy 3C 273

Alexandr Volvach [1,*], Larisa Volvach [1] and Mikhail Larionov [2]

[1] Radio Astronomy and Geodynamics Department of Crimean Astrophysical Observatory RAS, 298688 Katsively, Crimea
[2] Astro Space Center of Lebedev Physical Institute, Russian Academy of Sciences, 119991 Moscow, Russia
* Correspondence: rt22simeiz@yandex.com

Abstract: The data from the last 60 years on the programs of long-term multi-frequency monitoring of active galactic nucleus (AGN) 3C 273 were analyzed. A model is proposed for finding the parameters of close binary systems (CBSs) from supermassive black holes (SMBHs), including a harmonic analysis of observational data series obtained in the optical and radio ranges. The purpose of this research was to show that in the absence of optical information on AGNs, only radio data can be used and the necessary information on the physical objects can be obtained. Regarding the example of the blazar 3C 273, the following parameters were obtained: the masses of the companions; their orbital characteristics, such as the speeds of movement in orbits; the reserves of the kinetic energy of the system; and others. It was found that AGN 3C 273 can be a very massive binary system at the stage of evolution close to merging. Based on the obtained parameters, the characteristics of the gravitational waves (GWs) of this system, its lifetime before the merger, and the possible observation of 3C 273 using gravitational wave detectors were considered.

Keywords: active galactic nuclei; black holes; closed massive systems; gravitational waves

check for updates

Citation: Volvach, A.; Volvach, L.; Larionov, M. A Close Binary Supermassive Black Hole Model for the Galaxy 3C 273. *Galaxies* **2023**, *11*, 96. https://doi.org/10.3390/galaxies11050096

Academic Editors: Alberto C. Sadun and Atreya Acharyya

Received: 31 July 2023
Revised: 31 August 2023
Accepted: 3 September 2023
Published: 5 September 2023

1. Introduction

Active galactic nuclei (AGNs) contain supermassive black holes (SMBHs) in their central regions. At the end of the last century, it was suggested that these SMBHs form pairs [1]. We further emphasized that it is not just the duality of SMBHs in the central regions of the brightest AGNs that is important but also the close location of SMBHs to each other when they are at the stage of evolution close to merging. This is important not only from the point of view of obtaining a high level of energy release in the electromagnetic spectrum but also the significant emission of gravitational waves (GWs) [2–4].

AGN 3C 273, being the brightest representative of the family of quasars, or rather blazars, is one of the most studied objects. It has long been known as a wide-range emitter. Its observational history is about 60 years in the radio range and more than 110 years in the optical range. Being a relatively close object by space standards (z = 0.158, R = 630 Mpc), it is bright at all wavelengths. For example, in the optical range, its value is 12.9^{m}, and the bolometric luminosity is $6 \cdot 10^{46}$ erg s^{-1} [5].

This object has a pronounced flux density variability in a wide frequency range from fractions of hertz to nanohertz. The main parameters of this variability were established in the last century [6–8]. These characteristics include the detection of harmonic components in the long-term monitoring of AGN radiation flux densities on different time scales from a year to tens of years using harmonic analyses, which is needed to identify the orbital and precessional periods in a close binary (CB) supermassive black hole (SMBH) system. As shown below, these periods make it possible to obtain some of the most important parameters of the SMBH binary system.

A pronounced 13-year periodicity was observed in variations in the optical flux density of the blazar 3C 273 [6]. Furthermore, other periodic components were discovered.

A periodicity of 8.1 years was found at 15 GHz [9]. This was done by analyzing the radio light curve of 3C 273 at 15 GHz from 1963 to 2006 taken from a literature database. When analyzing a period of 13 years, optical data were collected from the end of the 20th century.

To establish the presence of orbital and precessional periods in the close SMBH system, it is necessary to have a long-term set of observational data covering many tens of years. In addition, some bright radio AGNs are sources that are weak in the optical range, for example, S 0528 + 134. In addition, a certain group of them also has powerful gas and dust complexes in their central regions. Absorption in the optical range from gas and dust can exceed 10^2 magnitudes [10]. In such a situation, relying only on the optical range is not necessary. A technique is needed that makes it possible to use other wavelength ranges, for example, the radio range, to determine the physical characteristics of double SMBHs. The advantages of the latter are undeniable in this particular situation.

At present, we probably have only two AGNs that presumably contain double SMBHs for which there are estimates of the parameters of these systems—OJ 287 and 3C 454.3 [11,12]. This is clearly insufficient for conclusions and generalizations about the physical characteristics of these important formations located in the central regions of galaxies, and any additional system of this kind whose characteristics have been determined from observations is important for understanding the processes occurring there.

In this study, we analyzed the multi-frequency data of the 3C 273 obtained in the radio and optical wavelength ranges over the past 60 years in order to obtain the parameters of this system based on the proposed model of binary supermassive black holes. In addition, the power of GWs emitted by the binary system was estimated, as well as other characteristics of the system associated with them.

2. Observations and Data Processing

Data at frequencies of 4.8 and 36.8 GHz were obtained using the 22 m radio telescope RT-22 of the Crimean Astrophysical Observatory and a radiometric system with diagram modulation [12]. Thus, it was possible to avoid the influence of the anomalous spectrum of fluctuations in the gains of the receivers on the observational data. The use of such a reception technique also made it possible to reduce signal fluctuations due to variations in the temperature of atmospheric inhomogeneities, which is significant in the centimeter and millimeter wavelength ranges. The antenna temperatures from the measured sources were obtained after subtracting the absorption of radiation by the Earth's atmosphere from them. Its value was determined as the difference between the signals from the output of the radiometer in two positions of the antenna when the radio telescope was pointed at the source alternately with one or the other receiving horn (signal reception technique on–on). This was carried out using the method of "atmospheric cuts" made every 3–4 h. With this procedure, the values of the antenna temperature were recorded at certain elevation angles of the radio telescope.

Source observations consisted of each measurement (on–on) repeated 5–20 times. Then, the mean value and standard error of the mean were calculated. The number of repetitions (on–on) was determined by the achievement of the required signal-to-noise ratio (at least 5) for each source. Calibration sources were observed, along with the objects under study, whose parameters are shown in Table 1.

Table 1. Flux densities for calibration sources at frequencies 4.8 and 36.8 GHz.

4.8 GHz	Source	3C 144	3C 274	M 17	3C 405
	Flux density, Jy	612.9	71.4	584.8	378.2
36.8 GHz	Source	DR 21	3C 274	NGC 7027	3C 286
	Flux density, Jy	18.3	14.3	5.1	1.56

When recalculating the antenna temperatures in the flux density, the dependence of the effective antenna area A_{eff} on the elevation angle h was also used in the calculations. The

A_{eff} values of the radio telescope, which were determined from the data of observations of calibration sources, were approximated using a dependence of the form

$$A_{eff} = a \cdot \sin h + b \cdot \cos h + c \quad (1)$$

where the coefficients a, b, and c were determined using the least squares method.

When calculating the root-mean-square error of the flux density, the antenna temperature measurement error σ_1 and the approximation error $A_{eff} - \sigma_2$ were taken into account. Typical values are σ_1 = (2–4)% and σ_2 = (3–6)%. With this data-processing technique, measurement errors were automatically included in the calculation due to the influences of equipment noise, telescope pointing errors, errors in determining the absorption coefficient, and instability of the radiometer gain.

Monitoring at frequencies of 8 and 14.5 GHz was performed using the 26 m RT-26 radio telescope of the University of Michigan Observatory in the period 1966 to 2012, the databases of which were previously published and used in the works [13,14]. Since 2012, observations at 8 GHz were also made using RT-22 in Katsiveli. Monitoring at a frequency of 15 GHz using the 40 m radio telescope of the Owens Valley Radio Observatory was made in the period 2013–2019 [15], as well as at a frequency of 36.8 GHz in Katsiveli (RT-22). Optical data was obtained using the Mercator telescope on La Palma (Canary Islands, Spain) [5,16,17] and the Frankfurt Quasar Monitoring Project by Stefan Karge (the Taunus Observatory of Physikalischer Verein, Frankfurt, Germany). Moreover, data was borrowed from the Open Science Observatories of the Open University (Milton Keynes, UK) using the COAST-Telescope (a 14-inch f/11 Schmidt-Cassegrain), the PIRATE-Telescope (a 17-inch f/6.8 Corrected Dall-Kirkham), the Bradford Robotic Telescope of the University of Bradford (Bradford, UK), and the Tzec Maun Observatory of the Tzec Maun Foundation (Cloudcroft, USA; a 14-inch f/3.8 Maksutov-Newton with ST-10XME/STL-6303 and a 16-inch f/9 16-inch f/9 Ritchey-Chrétien with STL-6303).

3. Results

The data of long-term monitoring of AGN 3C 273 in the radio and optical wavelength ranges are shown in Figure 1. We needed to obtain the main characteristics of the system from these observational data within the framework of the model of CB SMBHs. As was already mentioned, these main characteristics include the orbital and precessional periods and, of course, the SMBH masses. Based on these data, one can find the parameters of the SMBH orbits. An important characteristic of a system of close double SMBHs is the level of GWs coming from them and the lifetime of such systems before they merge.

Given the above, one of the important stages of our research was to obtain the harmonic components of the changes in the flux densities of AGN 3C 273 at all presented wavelengths. This led to the appearance of several combination frequencies in the analysis, including those responsible for the nutation period. These frequencies can be removed by introducing amplitude filtering, i.e., selecting harmonics that are more powerful. In addition, the amplitudes of the selected harmonics must in any case exceed five standard deviations.

With such remarks, the results were obtained by conducting a harmonic analysis using the Schuster method [14]. This method provides for the calculation of the Schuster periodogram $D(\omega)$, which is related to the true power spectrum $g(\omega)$ and the spectral window $W(\omega)$ using the following relationship [18]:

$$D(w) = \int_{-\infty}^{+\infty} g(w') \cdot W(w - w') dw' \quad (2)$$

This relationship can be used to "clean up" the spectrum, i.e., to remove unnecessary peaks associated with a finite and non-uniformly spaced time grid, as well as false maxima due to noise. We used the CLEAN technique, which is associated with the successive subtraction of all significant maxima from the "dirty" spectrum. Each subtracted spectral peak is defined by its complex amplitude, frequency, and spectral window, which depends on the distribution of the data over time. All subtracted peaks give a clean spectrum that is devoid of false maxima and noise. The spectrum is cleared until there are no peaks in the "dirty" spectrum that exceed a certain threshold level, which is determined by the probability of detecting a signal in the noise. With the help of spectral analysis algorithms, we revealed variations with different periods of the light curves of 3C 273. The data obtained using the CLEAN technique are presented in Tables 2 and 3. All values presented in Tables 2 and 3 correspond to peaks in the power spectrum above the 10σ level.

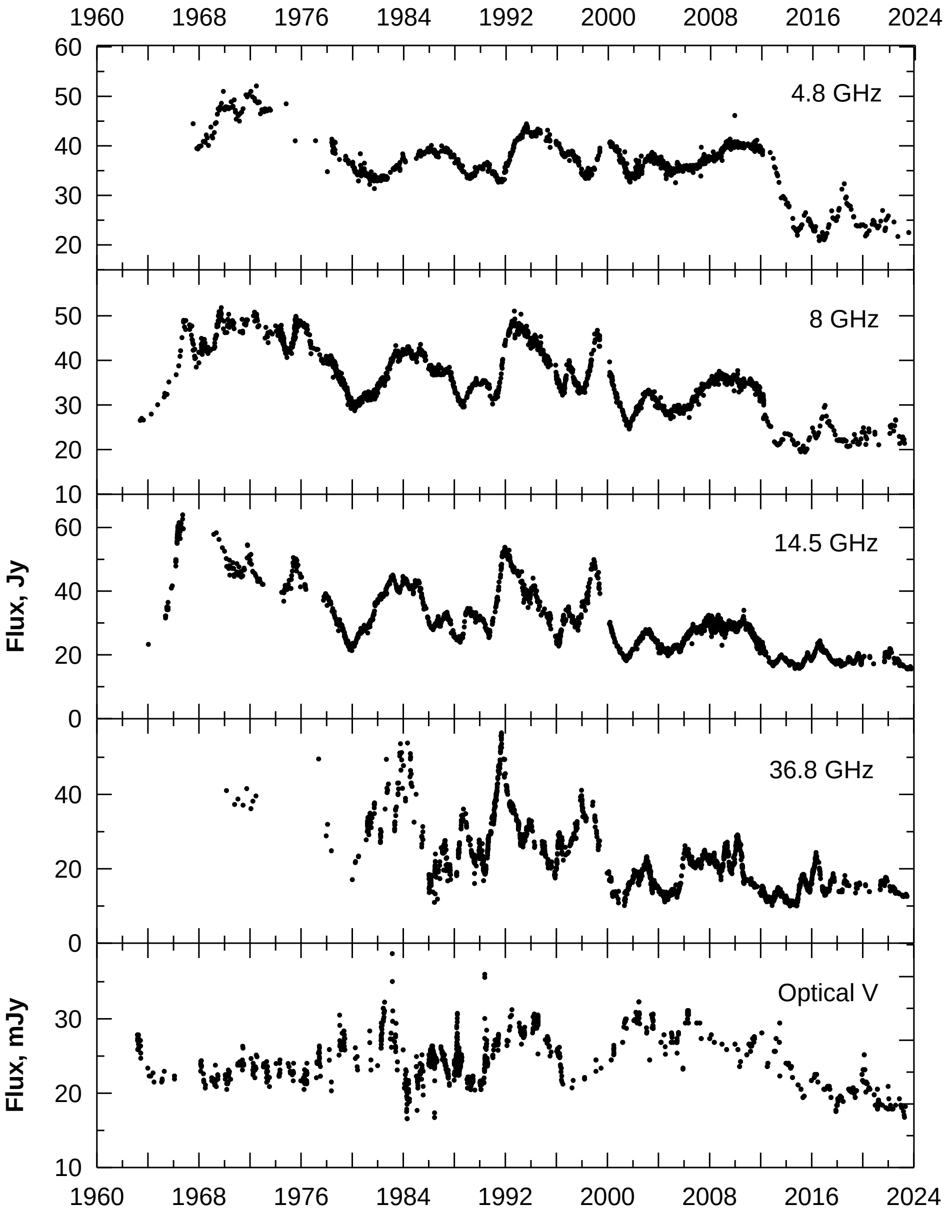

Figure 1. The data of multi-frequency long-term monitoring of AGN 3C 273 in the optical (V) and radio bands.

Table 2 shows the results of the harmonic analysis performed for all given frequencies in the radio and optical wavelength ranges.

The presence of a common set of close and, at the same time, strong harmonic components in the data of long-term multi-frequency monitoring of 3C 273 at radio and optical frequencies may indicate a single source of energy release, providing the appearance of alternating radiation in a wide wavelength range. This assumption is also evidenced by the type of delay between the frequencies of the received radiation, as shown below. This supports the fact that we receive radiation coming from a blazar from a narrow cone between the directions of the ejection (jet) and the observer. In this case, when propagating along the jet at each frequency, the source begins to become optically thin at different distances from its beginning. Since this occurs on scales less than a parsec, it is quite difficult to confirm this picture using direct interferometric methods for AGNs, which are at remote, cosmological distances.

Table 2. Results of harmonic analysis of multi-frequency monitoring of the 3C 273.

$T_{4.8GHz}$ (years)	12.6 ± 1.6 ($T_{pr,obs}$)	8.0 ± 0.9 (T_{obs})	5.2 ± 0.6 (T_{obs})	3.4 ± 0.5 ($T_{orb,obs}$)
T_{8GHz} (years)	12.0 ± 1.2 ($T_{pr,obs}$)	8.4 ± 0.8 (T_{obs})	5.0 ± 0.5 (T_{obs})	3.5 ± 0.4 ($T_{orb,obs}$)
$T_{14.5GHz}$ (years)	14.1 ± 1.2 ($T_{pr,obs}$)	8.3 ± 0.8 (T_{orb})	4.7 ± 0.5 (T_{obs})	3.6 ± 0.4 ($T_{orb,obs}$)
$T_{36.8GHz}$ (years)	14.5 ± 1.4 ($T_{pr,obs}$)	8.9 ± 0.8 (T_{obs})	5.0 ± 0.5 (T_{obs})	3.8 ± 0.5 ($T_{orb,obs}$)
$T_{Optical}$ (years)	10.6 ± 1.4 ($T_{pr,obs}$)		5.0 ± 0.5 (T_{obs})	2.9 ± 0.5 ($T_{orb,average}$)
$T_{average}$ (years)	13.3 ± 1.2 ($T_{pr,average}$)	8.4 ± 0.7 ($T_{average}$)	5.0 ± 0.4 ($T_{average}$)	3.5 ± 0.3 ($T_{orb,average}$)

The first column shows the names of the periods at various studied frequencies; the second, third, fourth, and fifth columns give the periods found at different frequencies, which are arranged in decreasing order, from precessional (13 years) periods to orbital (3.5 years) periods, through combinational (8.4 and 5.0 years) periods. The periods are specified in the frame of reference associated with the observer.

Table 3. Results of the harmonic analysis of multi-frequency monitoring of the 3C 273 for periods in the coordinate system associated with the source (Equation (3)).

$T_{4.8GHz}$ (years)	272 ± 30 ($T_{pr,ist}$)	172 ± 19 (T_{ist})	112 ± 13 (T_{ist})	73 ± 9 ($T_{orb,ist}$)
T_{8GHz} (years)	259 ± 25 ($T_{pr,ist}$)	181 ± 16 (T_{ist})	108 ± 10 (T_{ist})	76 ± 7 ($T_{orb,ist}$)
$T_{14.5GHz}$ (years)	304 ± 27 ($T_{pr,ist}$)	179 ± 15 (T_{ist})	101 ± 10 (T_{ist})	76 ± 7 ($T_{orb,ist}$)
$T_{36\cdot8GHz}$ (years)	313 ± 27 ($T_{pr,ist}$)	192 ± 17 (T_{ist})	108 ± 11 (Tist)	82 ± 8 ($T_{orb,ist}$)
$T_{Optical}$ (years)	229 ± 27 ($T_{pr,ist}$)		108 ± 11 (T_{ist})	63 ± 8 ($T_{orb,ist}$)
$T_{average}$ (years)	287 ± 20 ($T_{pr,average}$)	181 ± 17 ($T_{average}$)	107 ± 11 ($T_{average}$)	77 ± 5($T_{orb,average}$)

The first column shows the names of the periods at various studied frequencies; the second, third, fourth, and fifth columns give the periods found at different frequencies, which are arranged in decreasing order, from precessional (13 years) periods to orbital (3.5 years) periods, through combinational (8.4, 5.0 years) periods. The periods are given in the reference system associated with the radiation source.

From what has been said, it follows that we receive radiation from blazars from jets in all wavelength ranges from radio to optical, and thus, the periods are taken in the coordinate system associated with the source by using Equation (2) specified in the paper [19]:

$$T_{source} \approx \frac{T_{obs} \cdot \gamma^2}{1+z} \tag{3}$$

where γ is the gamma factor, the meaning of which and its relation to the duration of flare phenomena in blazars are considered in [20]. Taking into account the similarity of the flare activity of the 3C 273 and 3C 454.3 blazars in terms of the duration of the flares in them, we can assume the value γ = 5 for 3C 273, the same as for 3C 454.3 [12]. Then, the periods in the coordinate system associated with the source were recalculated in accordance with Equation (3) (Table 3).

The period of 13.3 years stands out. This period may be associated with precessional motions of the central SMBH (Table 2, sixth line). A short and powerful period of 3.5 years stands out at all frequencies. This is in accordance with the period of the companion's orbit (Table 2). The periodic component of 8.4 years, which is significant in amplitude, is located near the half-period of the precession of the central body (Table 2). Nutational movements can explain some of the shift in this period in the three-body system, where the role of the third body is played by a massive AD and accreting matter. The 5.0 years harmonic was present everywhere (Table 2). When combining it with a period of 8.4 years, we obtained exactly the harmonic of the precession half-cycle. The remaining harmonic components had a significantly lower amplitude. An example of the result of harmonic analysis of long-term monitoring data at all frequencies is shown in Figures 2–6.

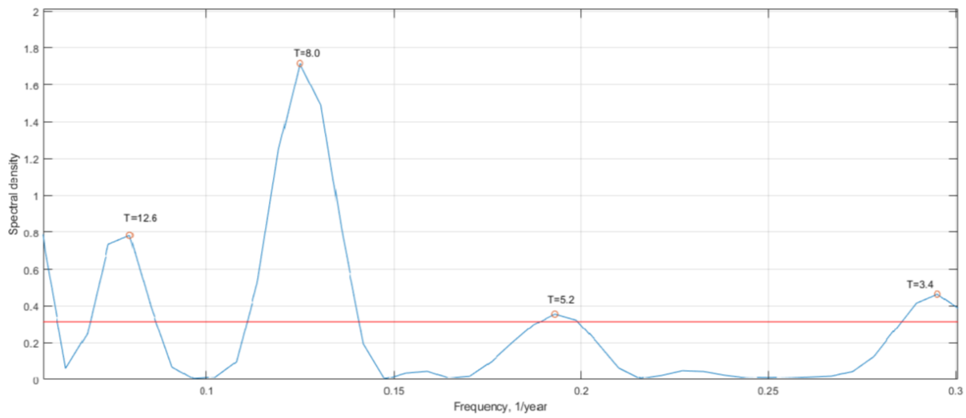

Figure 2. The result of harmonic analysis of long-term monitoring data at a frequency of 4 GHz. The horizontal line shows the 10-standard-deviation limit.

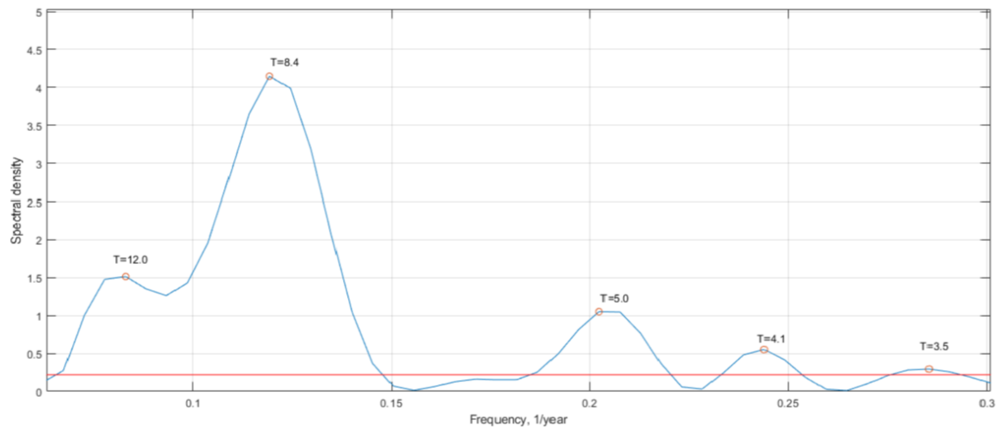

Figure 3. The result of harmonic analysis of long-term monitoring data at a frequency of 8 GHz. The horizontal line shows the 10-standard-deviation limit.

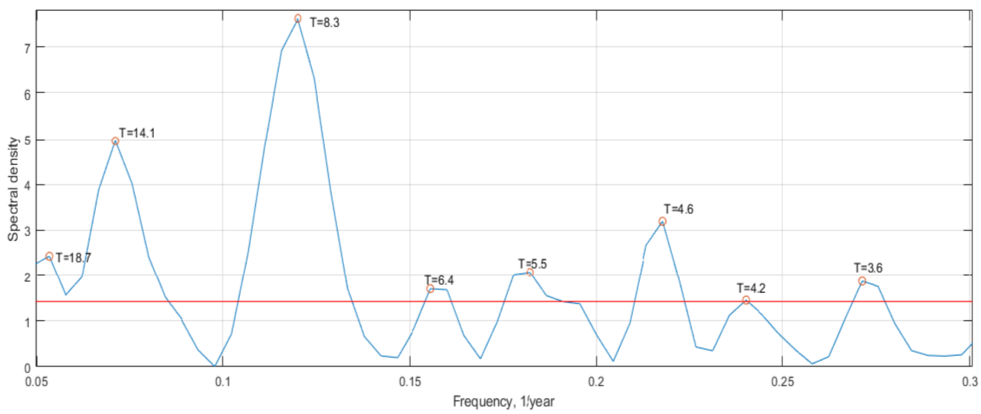

Figure 4. The result of harmonic analysis of long-term monitoring data at a frequency of 14.5 GHz. The horizontal line shows the 10-standard-deviation limit.

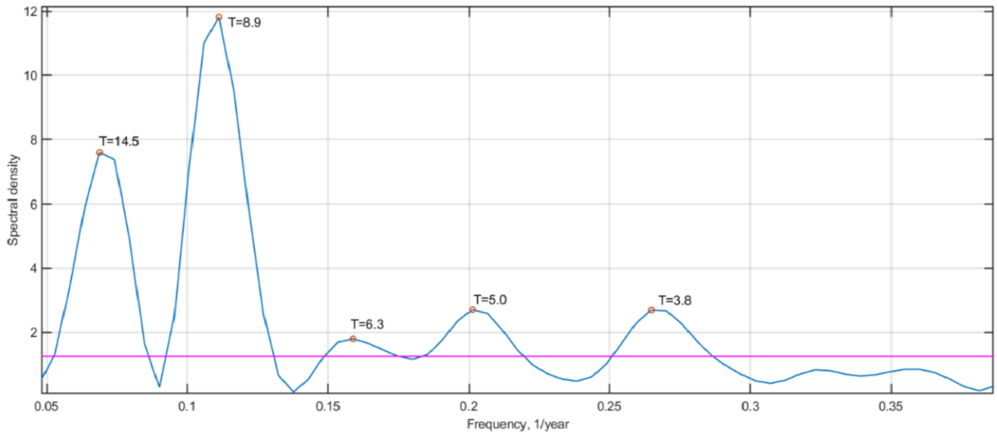

Figure 5. The result of harmonic analysis of long-term monitoring data at a frequency of 36 GHz. The horizontal line shows the 10-standard-deviation limit.

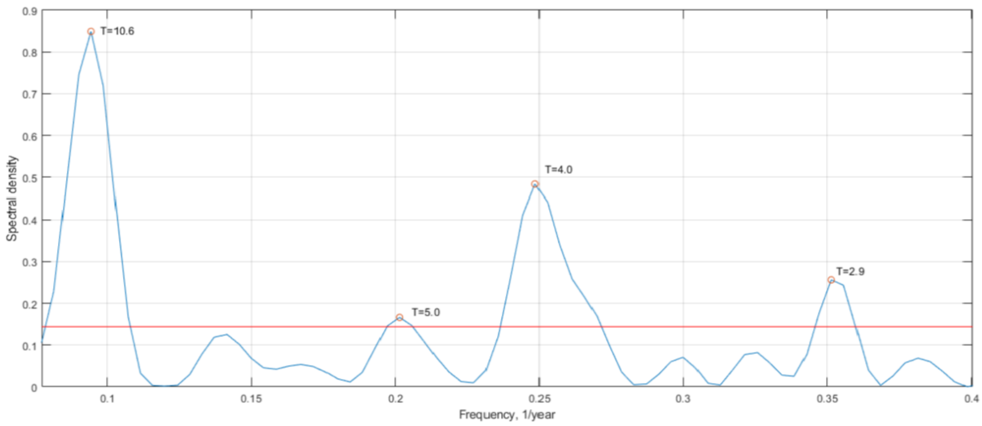

Figure 6. The result of harmonic analysis of long-term monitoring data in the optical range. The horizontal line shows the 10-standard-deviation limit.

Data from long-term multi-frequency monitoring of 3C 273 flux densities were used to determine the delays between different frequencies. To determine the delays between different wavelength ranges we used a discrete correlation function method [14].

At the beginning, close to the jet origin, there was a flare in the gamma range, and then we saw a flare in the X-ray range. These assumptions were based on the physical parameters of the medium near the origin jet, where temperatures can reach 5×10^9 K and the density is 10^9–10^{10} cm^{-3} [21]. After some months, we saw a flare in the optical wavelength range. Then, after 8.5 months, the flare was recorded in the millimeter wavelength range, and only then, years later, the flare manifested in the centimeter wavelength range (Figure 7). This type of delay dependence ruled out the possibility of their occurrence in a medium through which radiation propagates from the source. There, the frequency dependence is quite different. The method for determining the time delays between frequencies is described in [14].

It should be noted that we observed the delays of the flare phenomenon in the frame of reference associated with the observer. This did not include relativistic time interval corrections (Equation (3)).

Due to precessional motions in a binary SMBH system, there may be periods when the correlation between frequency bands is interrupted. Because of the different positions in space and time of the propagating "condensations in the jet" at different wavelength ranges, the correlation between them may disappear for a while. During the precession of the jet, there is a change in the Doppler factor for each wavelength range. Some other authors have also noted the "Fading" of correlation between different wavelengths.

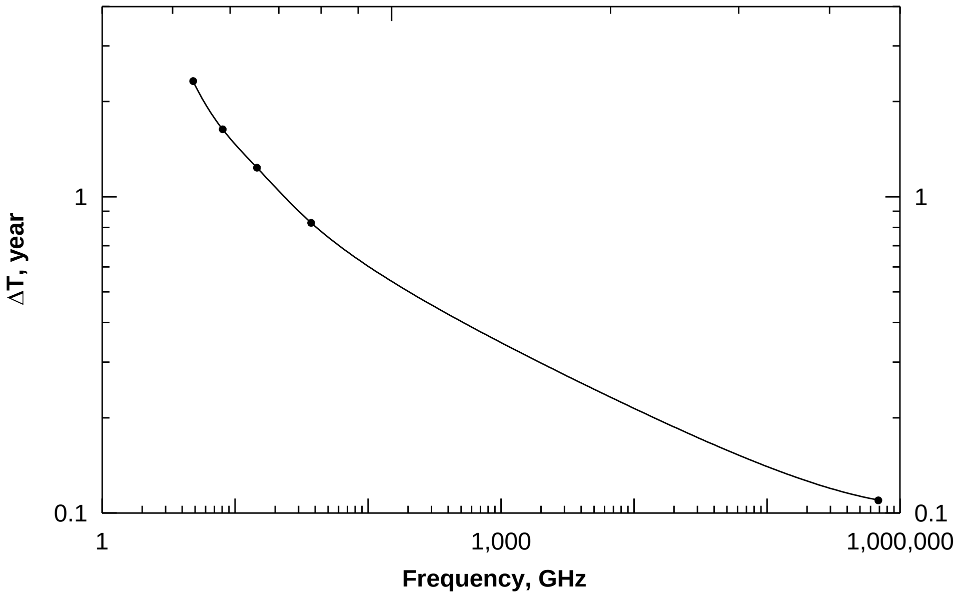

Figure 7. Time delays between the data of multi-frequency long-term monitoring AGN 3C 273 in the optical (V) and radio bands.

Nevertheless, we can even give data on 3C 273 in the gamma range, which correlates with the radio band (37 GHz) [22]. This indicates that they shared a common source of energy and, in this case, the radiation came from the jet component.

Data processing of the optical wavelength range showed the presence of harmonic components obtained in the radio range within the measurement errors, except for the periodic component of about 8 years. However, this periodic component was not used in our studies. More important was the conclusion that we could draw from the processing of data in the radio and optical range of wavelengths. If the optical counterpart of the object associated with the studied AGN was not visible, then we could safely carry out data processing in the radio range in order to obtain the characteristics of SMBH binary systems that are of interest to us. Such a situation can arise when the studied AGN is bright enough in the radio range and quite dim, or simply not visible, in the optical range. In addition to the already mentioned AGN S 0528 + 134, one can also note the well-known blzzar S5 0716 + 714. In addition, such cases are often encountered due to the considerable remoteness of AGNs and the presence of a dust component of matter in their central regions.

The precession of the central black hole, together with the central regions of the accretion disk from which ejections of relativistic matter occur, may occur due to perturbations from a massive companion moving with the orbital period T_{orb}. In accordance with the generalized Kepler's third law, we can write

$$m + M = \frac{4\pi^2 \cdot r^3}{G \cdot T_{orb}^2} \tag{4}$$

In this expression, m is the mass of the companion, M is the mass of the central black hole, r is the radius of the companion's orbit, and G is the gravitational constant. The angular velocity of the precession of the central black hole Ω_{pr} is determined from the ratio

$$\Omega_{pr} = \frac{3G \cdot m \cdot cos\imath}{4r^3 \cdot \omega}, \tag{5}$$

where ι is the half angle of the precession cone and ω is the angular velocity of the central SMBH rotation. Because Ω_{pr} =2π/T_{pr} and ω =2π/T_{rot}, the ratio (5) can be rewritten as

$$T_{rot}T_{pr} = \frac{16\pi^2 \cdot r^3}{3G \cdot m \cdot cos\iota}. \tag{6}$$

The right and left parts of relations (4) and (6) are divided by each other to obtain

$$\frac{M+m}{m} = 0.75\frac{T_{pr}}{T_{orb}} \tag{7}$$

We obtained that the mass function depends only on the ratio of precession and orbital periods.

From expressions (4) and (6), we found the masses of the central SMBH and the companion:

$$m = \frac{16\pi^2 \cdot r^3}{3G \cdot T_{orb} \cdot T_{pr}},\ M = \frac{16\pi^2 \cdot r^3 \cdot (0.75T_{pr} - T_{orb})}{3G \cdot T_{orb}^2 \cdot T_{pr}}. \tag{8}$$

These expressions also include the parameter R, which is the radius of the companion's orbit. The cubic dependence of the masses of companions on this important parameter should be noted. This means that the dimensions of the orbit can be in a rather narrow range of values that is limited by the possible mass from below and from above. The choice of a specific value of companion masses and orbit sizes is based on the physical conditions in the system. One of the important physical parameters of a binary SMBH system is its lifetime before merging. The estimated lifetime t_{merge} of the system before merging can be determined from the work [2]:

$$t_{merge} \approx \frac{2 \cdot 10^{-2} \cdot c^5 \cdot r^4 \cdot \left(1-e^2\right)^{\frac{7}{2}}}{G^3 \cdot m \cdot M \cdot (m+M)}\ \text{years}. \tag{9}$$

In this expression, m and M are the masses of the companions, e is the eccentricity of the companion's orbit, c is the speed of light, and G is the gravitational constant. We took e to be equal to zero. What physical conditions in CB systems of SMBHs led us to consider an orbit with e = 0? First, we had a close binary system with similar masses at the stage of evolution close to merging. Second, in galactic close binary massive star systems, the mass ratio of the components tends to 1 and the orbit becomes circular [23].

If we took the value $t_{merge} = 3 \cdot 10^5$, then taking into account (4, 6), we obtained the values of the companion orbit and SMBH masses equal to $R_{orb} \approx 4.5 \cdot 10^{17}$ cm, $m \approx 0.55 \cdot 10^{10}$ M_o, and $M \approx 1.0 \cdot 10^{10}$ M_o. With a decrease in the size of the companion's orbit, the lifetime of the system before merging swiftly decreased.

With the obtained parameters of the orbits of the CB SMBH system, the companions moved at high speeds: $v_{centr} \approx 10{,}570$ km s^{-1} and $v_{comp} \approx 14{,}300$ km s^{-1}. The kinetic energy reserve of the system was $W_k \approx 4.2 \cdot 10^{61}$ erg. Taking into account the lifetime of the system, the rate of average energy loss was dE/dt = $3 \cdot 10^{48}$ erg s^{-1}. This very large amount of energy was emitted in the form of GW and overcame dynamic friction against the dense environment of the AD, which began to play an important role in the SMBH system, through which the companions moved at high speed. In this case, the release of energy due to friction against a dense medium increased significantly.

We have very serious arguments in favor of the fact that the variability of the flux density in 3C 273 was not chaotic, but had signs of the presence of periodicities in its structure. This periodicity was justified by the presence of a complex of the most powerful harmonics present in all data of long-term multi-frequency monitoring. You cannot call it accidental; the probability of such an event is too insignificant.

Regarding the estimates of the mass of 3C 273 by other authors, any estimates can be made, but the resulting accuracy of three standard deviations is not very impressive. However, Paltani and Turler's optical/UV spectroscopy dynamic mass estimates differ by only 1.3 of their standard deviations from our central SMBH estimates [24]. They obtained $M_{BH} \approx 6.6 \cdot 10^9$ M_o against our $M_{SMBH} \approx 10^{10}$ M_o. One can speak of good agreement between the data.

We can talk about some arbitrariness in the choice of t_{merge} for 3C 273. Let us say the following about this. We cannot change this value in one direction or another by more than one and a half times. This does not allow us to identify a definite balance between the masses of the companions and the dimensions of the companion's orbit (the denominator and numerator of Equation (9)). In the numerator and denominator, there are large powers in the quantities of interest to us.

It would be interesting to obtain data on the AD, which may be common in the case of CB SMBHs. Observational evidence of such a possibility was already obtained by us in [12]. AD parameters can be estimated using the central body precession formula [25]:

$$T_{pr} \approx 10^6 \sqrt{\frac{M+m}{10^9\ M_o}} \cdot \left(1.8 \cdot \frac{R_{orb}}{10^{19}}\right)^3 \cdot \frac{R_{ad}}{10^{18}}^{-\frac{3}{2}} \cdot \frac{\sqrt{\frac{M+m}{M}}}{\frac{m}{M}} \text{ years.} \tag{10}$$

where $q = m/M$, $a = R_{comp} + R_{centr} = R_{comp} + (m \cdot v_{orb} \cdot R_{comp})/M \cdot v_{cent} = 1.8 \cdot R_{orb}$ is the distance between the companions, R_{ad} is the radius of the AD, and i is the angle between the orbital and AD planes (half angle of the precession cone). For blazars, i is less than 20°, and thus, we could take cos i = 1. Therefore,

$$R_{ad} \approx 10^{22} \cdot \left(\frac{M+m}{10^9 M_o}\right)^{\frac{1}{3}} \cdot \left(1.8 \cdot \frac{R_{orb}}{10^{19}}\right)^2 \cdot \frac{\left(\frac{M+m}{M}\right)^{\frac{1}{3}}}{\left(T_{pr} \cdot \frac{m}{M}\right)^{\frac{2}{3}}} \tag{11}$$

Substituting in formula 11, the period of the precession $T_{pr} \approx 287$ years (Table 3), masses of the companions ($m \approx 0.55 \cdot 10^{10}$ M_o, $M \approx 1 \cdot 10^{10}$ M_o), $R_{orb} = 4.5 \cdot 10^{17}$ cm, i = 0, and q = 0.55, we obtained the value $R_{ad\ 3C273} \approx 2$ pc. Thus, the radius of the AD was several times greater than the radius of the companion's orbit. When the plane of the AD coincided with the plane of the orbits of the companions, they practically moved inside the AD in its dense medium. This can be seen in multi-frequency monitoring (Figure 1) in the form of increases in flux densities due to the corresponding phases of the precession period. We observed this pattern if we assumed the presence of flares when the companions of the AD plane crossed twice per orbital period

Summing up, it can be noted that one of the brightest AGNs 3C 273 is a massive, close SMBH binary system, which is at the stage of evolution close to merging. In terms of the rate of energy loss, this system is comparable to the brightest blazar 3C 454.3 [12].

4. Discussion

The companions of the CBS SMBH system 3C 273 revolve around a common center of gravity, which spends a considerable amount of time inside the common AD for both of them. Based on the data obtained in our model for 3C 273 ($a = R_{comp} + R_{centr} = 1.8 \cdot R_{orb}$), $m = 0.55 \cdot 10^{10}$ M_o, $M = 1.0 \cdot 10^{10}$ M_o, and $R_{orb} = 4.5 \cdot 10^{17}$ cm, it was possible to calculate the rate of energy loss due to the radiation of GWs, while taking e = 0 [2]:

$$\langle \frac{dE}{dt_{3C273}} \rangle = \frac{32 \cdot G^4 \cdot M^2 \cdot m^2 (M+m) \cdot \left(1 + \frac{73e^2}{24} + \frac{37e^4}{96}\right)}{5c^5 \cdot a^5 (1-e^2)^{\frac{7}{2}}} > 0.3 \cdot 10^{47} \frac{erg}{s}. \tag{12}$$

To determine the parameters of the 3C 273, we used a slightly modified approach compared with 3C 454.3 [12]. It will be interesting to compare our data with those known for the blazar 3C 454.3. It turns out that despite the difference in the obtained masses of the companions and the distance between them, the value of the companion's orbit remained about the same. This is why, the GW losses for our two blazars were determined by the difference in the masses of the SMBH companions entering them. As a result, 3C 454.3's

GW losses were 25 times greater than those of 3C 273. But it remained a powerful source of GWs.

In the case of another bright blazar, namely, OJ 287, for which the physical characteristics of the SMBH binary system were determined via observations, the following can be noted. This double system can be used for the detection of GWs [11,26]. The angular momentum of OJ 287 is lost in the process of strong GWs and electromagnetic radiation, which also leads to a short lifetime of only about tens of thousands of years. This is close to our data for 3C 454.3 and 3C 273.

Another important feature of the blazars 3C 454.3 and 3C 273 could be noted in comparison with OJ 287. Both of our objects could be located within the AD for a long time, which provides increased dynamic friction in the system and energy release. During the AD precession, SMBH companions were located in different parts of AD, where the density and inhomogeneity differed. The energy loss of the system due to dynamic friction could be a significant, if not the main part, together with the GW radiation. These processes greatly reduced the lifetime of the system before merging.

The radiation of 10^{47} erg s^{-1} in the form of GWs must inevitably affect the parameters of the orbits of the SMBH companions. The distance between companions should decrease. To determine the magnitude of the change in the orbits of the 3C 273 companions and the possibility of experimental measurement of this, we calculated the rate of orbit decrease using the following formula [2]:

$$\langle \frac{da}{dt} \rangle \approx 64 \cdot G^3 \cdot M \cdot m \cdot (M+m) \cdot \frac{1 + \frac{73e^2}{24} + \frac{37e^4}{96}}{5c^5 \cdot a^3} \approx 2.1 \cdot 10^1 \frac{cm}{s} \quad (13)$$

where G is the gravitational constant, M and m are the masses of companions ($m = 0.55 \cdot 10^{10}$ M_o, $M = 1.0 \cdot 10^{10}$ M_o), $R_{orb} = 4.5 \cdot 10^{17}$ cm, $a = 8 \cdot 10^{17}$ cm, and $e = 0$.

The change in the companion's orbit was $\Delta R \approx 2.0 \cdot 10^1$ cm s^{-1}. The same for only one orbital period was $\Delta R_{Torb} \approx 0.5 \cdot 10^{11}$ cm. Over 17 observation periods (60 years/3.5 years = 17), the orbit decreased by 10^{12} cm, which corresponded to a decrease in the orbital period ΔT_{nep} by less than a tenth of a day. This value was much less of the error in determining the period (Table 2) and the accuracy of determining the time of a flare, the duration of which can be a year or more.

5. Conclusions

1. A method for calculating the parameters of the orbits of close binary SMBHs using only multi-frequency monitoring data in the radio range was considered. The long-term multi-frequency monitoring data used covered 60 years.
2. The physical parameters of close binary SMBHs included the masses of SMBH companions, the kinematic and dynamic parameters of their orbits, the kinetic energy of the system, and the lifetime before merging.
3. The data of harmonic analysis in the radio and optical ranges corresponded to each other, which made it possible to perform the necessary studies of objects based only on radio data when the optical counterparts of the AGN were not visible. This made it possible to significantly expand the range of sources under study.
4. An estimate was made of the size of the accretion disk of the SMBH system, which became common for both SMBHs at the stage of evolution close to the merger.
5. Estimates of the level of GW coming from 3C 273 show that 3C 273 can currently be the most powerful GW emitter, along with 3C 454.3. Due to the closer distance compared with 3C 454.3, it provides the highest level of GW flux density on the Earth's surface.
6. Like two other blazars, namely, 3C 454.3 and OJ 287, 3C 273 is a short-lived source with a lifetime of one hundred thousand years.
7. According to the obtained physical characteristics, 3C 273 is the most promising source for determining the gravitational waves coming from it using International Pulsar Timing Array gravitational wave detectors.

8. Using this method, identifying changes in the orbits of 3C 273 companions due to GW radiation is not yet possible, because these changes are far beyond the possibility of their experimental determination.

Author Contributions: A.V., L.V. and M.L.: conceived and designed the experiments, performed the experiments, analyzed and interpreted the data, and wrote the paper. All authors have read and agreed to the published version of the manuscript.

Funding: This research was funded by the Russian Science Foundation, grant number 23-22-10032.

Data Availability Statement: Data are contained within the article.

Acknowledgments: This study used data from the OVRO 40 m radio telescope monitoring program, which is partially supporting by NASA grants NNX08AW31G, NNX11A043G, NNX14AQ89G, and NSF, as well as grants AST-0808050 and AST-1109911. The optical data was from the Frankfurt-based Steffan Karger quasar-monitoring project. We thank a referee for their efforts to improve the quality of the manuscript.

Conflicts of Interest: The authors declare no conflict of interest.

References

1. Sillanpaa, A.; Takalo, L.O.; Pursimo, T.; Lehto, H.J.; Nilsson, K.; Teerikorpi, P. Confirmation of the 12-year optical outburst cycle in blazar OJ 287. *Astron. Astrophys.* **1996**, *305*, 17–20.
2. Peters, P.C. Gravitational radiation and the motion of two point masses. *Phys. Rev.* **1964**, *136*, B1224–B1232. [CrossRef]
3. Turner, M. Gravitational radiation from point-masses in unbound orbits: Newtonian results. *Astrophys. J.* **1977**, *216*, 610–619. [CrossRef]
4. Fernandez, J.J.; Kobayashi, S. Black hole mergers induced by tidal encounters with a galactic centre black hole. *MNRAS* **2019**, *487*, 1200–1209. [CrossRef]
5. Soldi, S.; Türler, M.; Paltani, S.; Aller, H.D.; Aller, M.F.; Burki, G.; Chernyakova, M.; Lähteenmäki, A.; McHardy, I.M.; Robson, E.I.; et al. The multiwavelength variability of 3C 273. *Astron. Astrophys.* **2008**, *486*, 411–425. [CrossRef]
6. Smith, H.J.; Hoffleit, D. Light Variations in the Superluminous Radio Galaxy 3C273. *Nature* **1963**, *198*, 650–651. [CrossRef]
7. Jurkevich, I. On the Light Variation of the Quasar 3c 273. *Astrophys. J.* **1972**, *172*, 29–33. [CrossRef]
8. Abraham, Z.; Romero, G.E. Beaming and precession in the inner jet of 3C 273. *Astron. Astrophys.* **1999**, *344*, 61–67.
9. Zhang, H.-J.; Zhao, G.; Zhang, X.; Bai, J.-M. The periodicity of 3C 273's radio light curve at 15 GHz found by the wavelet method. *Sci. China Phys. Mech. Astron.* **2010**, *53*, 252. [CrossRef]
10. Wilking, B.A.; Gagné, M.; Allen, L. E Star Formation in the ρ Ophiuchus Molecular Cloud. In *Handbook of Star Forming Regions*; Bo, R., Ed.; The Southern Sky ASP Monograph Publications: San Francisco, CA, USA, 2008; Volume 5, p. 351.
11. Valtonen, M.J. New Orbit Solutions for the Precessing Binary Black Hole Model of OJ 287. *ApJ* **2007**, *659*, 1074. [CrossRef]
12. Volvach, A.E.; Volvach, L.N.; Larionov, M.G. Most massive double black hole 3C 454.3 and powerful gravitational wave radiation. *Astron. Astrophys.* **2021**, *648*, A27. [CrossRef]
13. Aller, M.F.; Aller, H.D.; Hughes, P.A. The Longterm Centimeter-band Total Flux and Linear Polarization Properties of the Pearson-Readhead Survey Sources. *Bull. Am. Astron. Soc.* **2001**, *33*, 1516.
14. Vol'vach, A.E.; Kutkin, A.M.; Vol'vach, L.N.; Larionov, M.G.; Lakhteenmaki, A.; Tornikoski, M.; Nieppola, E.; Tammi, J.; Savolainen, P.; Leon-Tavares, J.; et al. Results of Long-Term Monitoring of 3C 273 over a Wide Range of Wavelengths. *Astron. Rep.* **2013**, *57*, 34–45. [CrossRef]
15. Richards, J.L.; Max-Moerbeck, W.; Pavlidou, V.; King, O.G.; Pearson, T.J.; Readhead, A.C.; Reeves, R.; Shepherd, M.C.; Stevenson, M.A.; Weintraub, L.C.; et al. Blazars in the Fermi Era: The OVRO 40 m Telescope Monitoring Program. *ApJS* **2011**, *194*, 29. [CrossRef]
16. Türler, M.; Paltani, S.; Courvoisier, T.-L.; Aller, M.F.; Aller, H.D.; Blecha, A.; Bouchet, P.; Lainela, M.; McHardy, I.M.; Robson, E.I.; et al. 30 years of multi-wavelength observations of 3C 273. *Astron. Astrophys. Suppl. Ser.* **1999**, *134*, 89–101. [CrossRef]
17. Türler, M.; Chernyakova, M.; Courvoisier, T.J.-L.; Foellmi, C.; Aller, M.F.; Aller, H.D.; Kraus, A.; Krichbaum, T.P.; Lähteenmäki, A.; Marscher, A.; et al. A historic jet-emission minimum reveals hidden spectral features in 3C 273. *Astron. Astrophys.* **2006**, *451*, L1–L4. [CrossRef]
18. Vityazev, V.V. Time series analysis of unequally spaced data: The statistical properties of the Schuster periodogram. *Astron. Astrophys. Trans.* **1996**, *11*, 159–173. [CrossRef]
19. Rieger, F.M. Supermassive binary black holes among cosmic gamma-ray sources. *Astrophys. Space Sci.* **2007**, *309*, 271–275. [CrossRef]
20. Vol'vach, A.E.; Larionov, M.G.; Kardashev, N.S.; Lähteemmäki, A.; Tornikoski, M.; Hovatta, T.; Nieppola, E.; Torniainen, I.; Aller, M.F.; Aller, H.D. A Multi-Frequency Study of Brightness Variations of the Blazar 0716+714. *Astron. Rep.* **2009**, *53*, 777–784. [CrossRef]

21. Volvach, A.E.; Volvach, L.N.; Larionov, M.G.; Aller, H.D.; Aller, M.F.; Raiteri, K.M. Correlations Between the Development of a Flare in the Blazar 3C 454.3 in the Radio and Optical. *Astron. Rep.* **2008**, *52*, 867–874. [CrossRef]
22. Esposito, V.; Walter, R.; Jean, P.; Tramacere, A.; Türler, M.; Lähteenmäki, A.; Tornikoski, M. The high energy spectrum of 3C 273V. *Astron. Astrophys.* **2015**, *576*, A122. [CrossRef]
23. Chini, R.; Hoffmeister, V.H.; Nasseri, A.; Stahl, O.; Zinnecker, H. A spectroscopic survey on the multiplicity of high-mass stars. *MNRAS* **2012**, *424*, 1925–1929. [CrossRef]
24. Paltani, S.; Turler, M. The mass of the black hole in 3C 273. *Astron. Astrophys.* **2005**, *435*, 811–820. [CrossRef]
25. Dunn, R.J.H.; Fabian, A.C.; Sanders, J.S. Precession of the super-massive black hole in NGC 1275 (3C 84)? *MNRAS* **2006**, *366*, 758–766. [CrossRef]
26. Dey, L.; Gopakumar, A.; Valtonen, M.; Zola, S.; Susobhanan, A.; Hudec, R.; Pihajoki, P.; Pursimo, T.; Berdyugin, A.; Piirola, V.; et al. The Unique Blazar OJ 287 and Its Massive Binary Black Hole Central Engine. *Universe* **2019**, *5*, 108. [CrossRef]